

Achieving Small Structures in Thin NiTi Sheets for Medical Applications with Water Jet and Micro Machining: A Comparison

M. Frotscher, F. Kahleyss, T. Simon, D. Biermann, and G. Eggeler

(Submitted May 11, 2010; in revised form October 19, 2010)

NiTi shape memory alloys (SMA) are used for a variety of applications including medical implants and tools as well as actuators, making use of their unique properties. However, due to the hardness and strength, in combination with the high elasticity of the material, the machining of components can be challenging. The most common machining techniques used today are laser cutting and electrical discharge machining (EDM). In this study, we report on the machining of small structures into binary NiTi sheets, applying alternative processing methods being well-established for other metallic materials. Our results indicate that water jet machining and micro milling can be used to machine delicate structures, even in very thin NiTi sheets. Further work is required to optimize the cut quality and the machining speed in order to increase the cost-effectiveness and to make both methods more competitive.

Keywords micro milling, NiTi, pseudoelasticity, shape memory alloys, stents, water jet machining

1. Introduction

Small structures in NiTi shape memory alloys (SMA) are commonly manufactured by laser cutting techniques. Unfortunately, one of the key disadvantages of these methods is the thermal interaction with the work piece through the formation of heat affected zones (HAZ). SMAs are especially sensitive to this kind of interactions, because phase transformation temperatures can be changed and extensive and costly postprocessing may be required. We examine two alternative processing methods, where the thermal influence on the material is negligible or not existent. Water jet machining can be used to economically cut structures in hard-to-machine materials. Micro machining uses very small tools, so that the contact area to the work piece is minimal. The goal of this study was to compare key aspects between the two processing techniques, such as traverse speed, cutting width, and cut quality. The microstructure was analyzed by scanning electron microscopy (SEM) and transmission electron microscopy (TEM) before and after cutting. In order to examine the cutting edges of water jet-machined sheets focused ion beam (FIB) was used to prepare TEM samples.

This article is an invited paper selected from presentations at Shape Memory and Superelastic Technologies 2010, held May 16–20, 2010, in Pacific Grove, California, and has been expanded from the original presentation.

M. Frotscher, T. Simon, and G. Eggeler, Institute for Materials, Ruhr-University Bochum, Bochum, Germany; and **F. Kahleyss** and **D. Biermann**, TU Dortmund, Institute of Machining Technology, Dortmund, Germany. Contact e-mail: matthias.frotscher@rub.de.

2. Experimental

2.1 Material

In this study, binary pseudoelastic NiTi sheets (380×80 mm) with a Ni-content of 50.9 at.% and a thicknesses of $s = 0.1$ mm (oxide free surface) were examined. The material was obtained from Memry GmbH, Weil am Rhein, Germany. Differential scanning calorimetry (DSC) was performed, using a DSC Netzsch type CC 204 F1 to determine the phase transformation temperatures as described in Ref 1. The material exhibits a two-step martensitic transformation on cooling from room temperature and a one-step reverse transformation back to austenite on heating.

2.2 Water Jet Machining

We used a water jet system Maximator JET type JETMax HS 0610 with a 37 kW pressure pump and a maximum nominal pump pressure of 400 MPa. Abrasive cutting was performed with SiO_2 abrasive (mass flow rate $m_a = 25$ g/min, mesh #120 and #220) at $p = 50\text{--}380$ MPa. Non-abrasive precision water jet machining made use of a collimator tube type 3DS and sapphire nozzles with a focusing diameter of $d_n = 0.08$ mm. The stand-off distance between the work piece and the nozzle was $S_D = 2\text{--}8$ mm. The NiTi sheets were mounted between two sheets of steel with a thickness of 2 mm and “cutting windows.” This sandwich-like setup prevents damage to the sensitive surfaces and reduces the risk of bending.

2.3 Micro Milling

The cutting tools were solid carbide end mill cutters with a diameter of 0.4 mm. The tools were coated with a thin TiAlN layer. The milling experiments were conducted on a CNC machine tool Kern HSPC 2522. The high-frequency spindle offers a speed range of 15,000–60,000 rpm. The experiments

were performed with ester oil for minimum quantity lubrication (MQL). The machine tool was located in an air-conditioned room in order to separate the micro milling process from vibrations, dirt, and thermal fluctuation. The cutting speed was varied in a range of $v_c = 25\text{-}37 \text{ m/min}$. The feed speed was constant at $v_T = 131 \text{ mm/min}$, which corresponds to a feed rate per tooth of $f_z = 4.5\text{-}6.5 \mu\text{m}$. The cutting depth was increased from $a_p = 10$ to $100 \mu\text{m}$.

2.4 Microstructural Analysis

The surface quality was analyzed using a SEM Jeol type JSM-840A at an acceleration voltage of 25 kV . Secondary phases were characterized by energy dispersive x-ray analysis (EDX) (micro-analysis unit of type EDAX Phoenix). Microstructures were analyzed in a TEM FEI type Tecnai F20 G² and TEM samples were prepared using a FIB FEI type Quanta 200 3D, Fig. 1.

3. Results and Discussion

3.1 Adaptation of the Water Jet Cutting Processes for Stent-Like Structures in Thin NiTi Sheets

The traverse speed v_T has a major impact on the cut quality. Abrasive water jet machining of small structures requires so-called fine cutting with a traverse speed of $9\text{-}30 \text{ mm/min}$ for machining of 1 and 0.5 mm NiTi sheets. However, a traverse speed of 22 mm/min seems to be the upper limit with regard to penetration and cut quality for a pump pressure of 350 MPa . This is in good accordance with work on Ti6Al4V (Ref 2).

The machining of NiTi sheets with abrasive leads to the rounding of the cut edge and a geometrically well-defined cut edge, Fig. 2. However, there is an area of $<500 \mu\text{m}$, which is influenced by the abrasive particles. This area can be subdivided into three zones: (1) the zone closest to the cut shows the rounding of edges and a strong influence of the water jet with signs of plastic deformation; (2) an impact zone, where the effect of the blast is still optically visible; and (3) the zone farthermost from the cut edge, which is little influenced by the blast, but still shows individual particle marks.

SEM analysis showed that abrasive particles can be found embedded in the NiTi surface after water jet machining, Fig. 3. These particles were identified as carbides of type SiC.

The achievable cutting width c_w for abrasive water jet machining at $p = 350 \text{ MPa}$ and a stand-off distance of $S_D = 3 \text{ mm}$ was determined to 0.68 mm (orifice/nozzle combination of $d_o/d_n = 0.5/0.17 \text{ mm}$). Abrasive water jet machining of sheet thicknesses below 0.5 mm was not satisfactory because small structures are blown away and bending of edges occurs.

Non-abrasive water jet machining of 0.1 mm sheets at 350 MPa leads to acceptable results for NiTi with regard to quality and structure size at a traverse speed of $3\text{-}9 \text{ mm/min}$. Machining at $p = 300 \text{ MPa}$, using a collimator tube and $d_n = 0.08 \text{ mm}$ nozzles, leads to a cutting width of $c_w = 0.15\text{-}0.21 \text{ mm}$ and strut widths of $b = 0.2\text{-}0.3 \text{ mm}$. However, the surface of thin pseudoelastic NiTi sheets is strongly influenced by the pure water jet close to the cut edge, Fig. 4. There is a difference between the front and the backside of the sheet with regard to the amount of plastic deformation. On the reverse side of the sheet chunks of material have been blown away, due to the nature of the jet geometry.

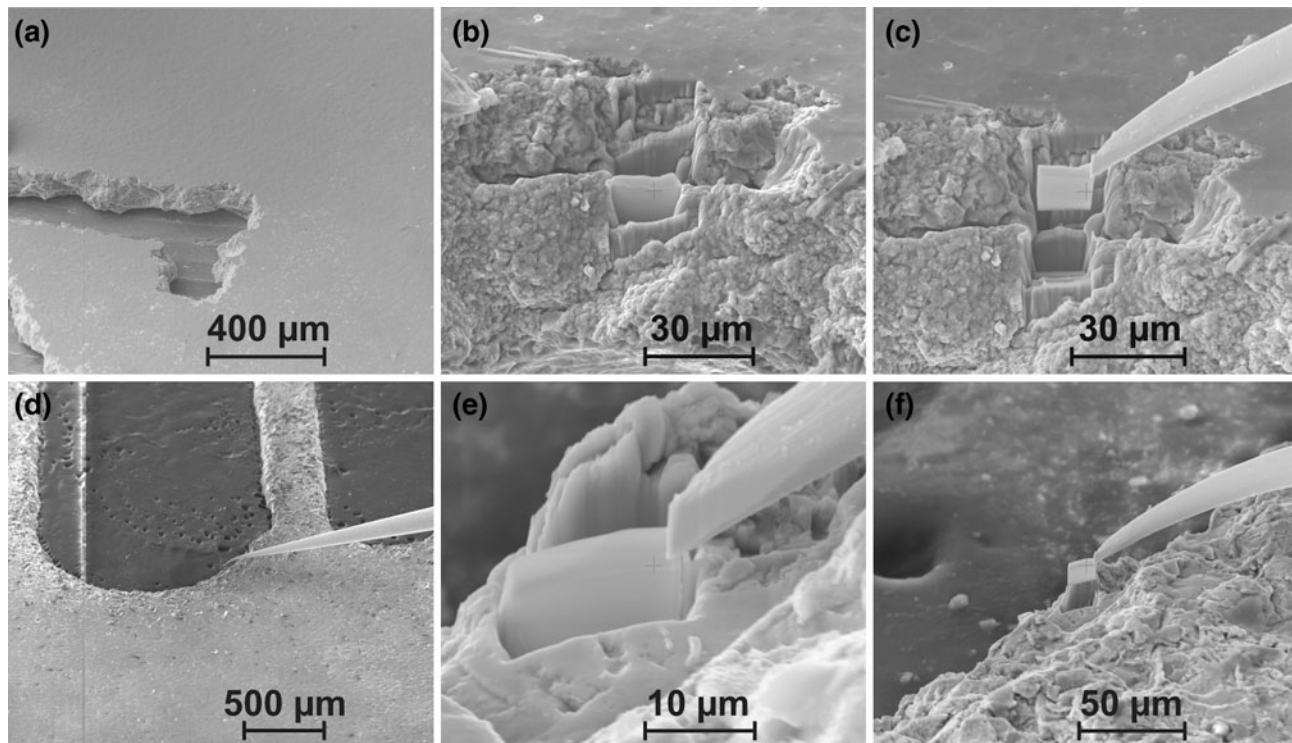


Fig. 1 Sequence of SEM images showing the FIB preparation of TEM samples taken out of the cut edge of a thin NiTi sheet machining by water jet

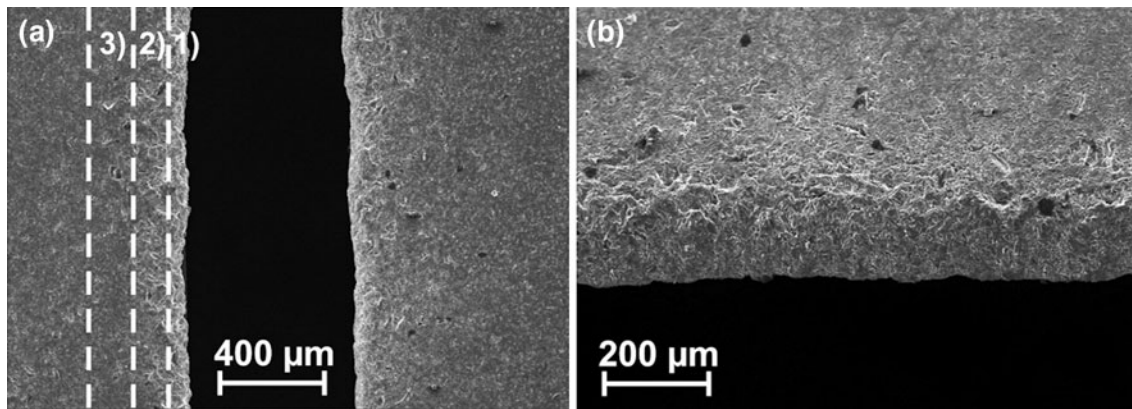


Fig. 2 Cut edge quality of a thin NiTi sheet machined with abrasive water jet as observed in the SEM

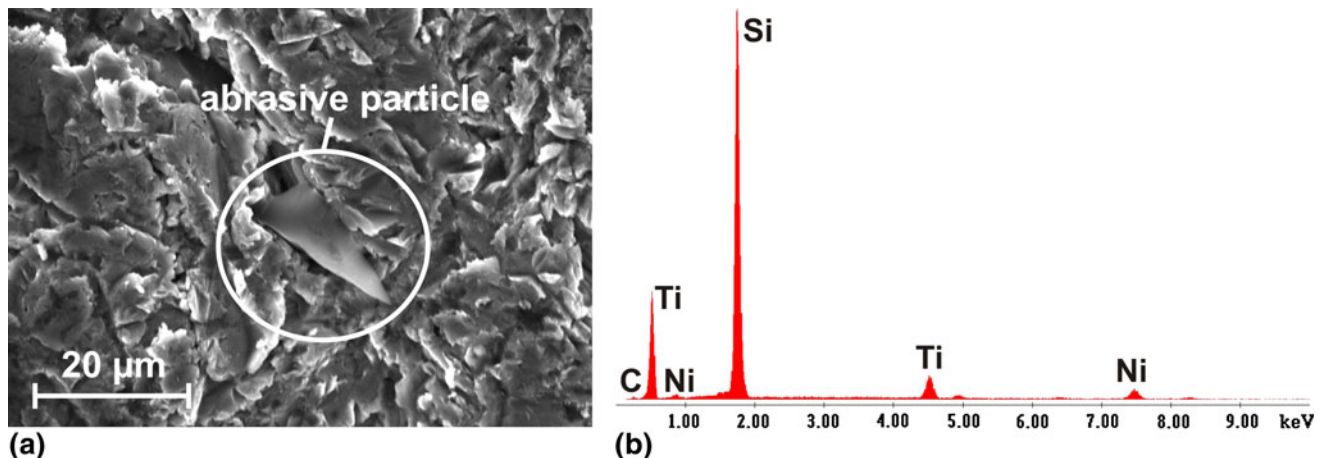


Fig. 3 SEM image and EDX spectrum of abrasive particles embedded in the NiTi surface in a zone along the cut edge after abrasive water jet machining

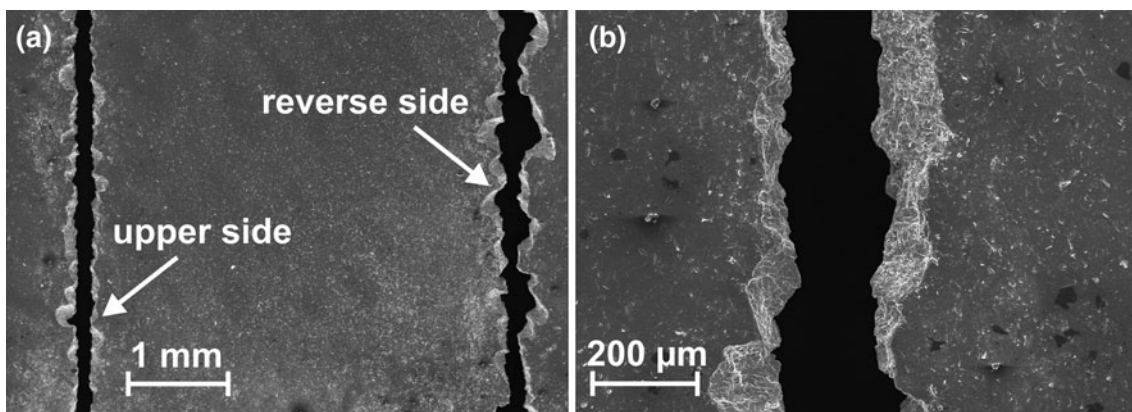


Fig. 4 SEM image showing the difference between the front and backside surfaces of a thin NiTi sheet machined with non-abrasive water jet

SEM investigations of the cut edge revealed heavy plastic deformation and the presence of small microcracks (white arrows in Fig. 5b). In contrast to abrasive water jet machining, the zone influenced by the blast is much smaller.

The cut edge quality of NiTi sheets with a thickness of 0.1 mm, machined by pure water jet should be improved. Most likely the thin sheets start to vibrate due to pressure fluctuation of ± 50 MPa in the high pressure system. However,

non-abrasive water jet machining allows the cutting of delicate structures with a cutting width in the order of 0.2 mm. Further work is required to improve the cut quality.

3.2 Microstructural Analysis of the Peripheral Zone

The microstructure of 0.1 mm NiTi sheets was investigated in the TEM. Figure 6 shows TEM brightfield images of the

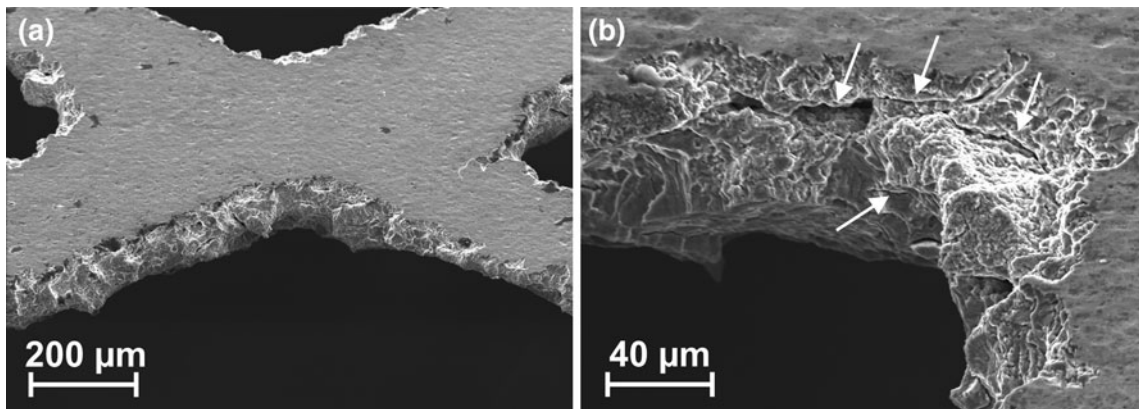


Fig. 5 SEM image of a small structure machined into a thin NiTi sheet with non-abrasive water jet. Microcracks in the cut edge are indicated by arrows

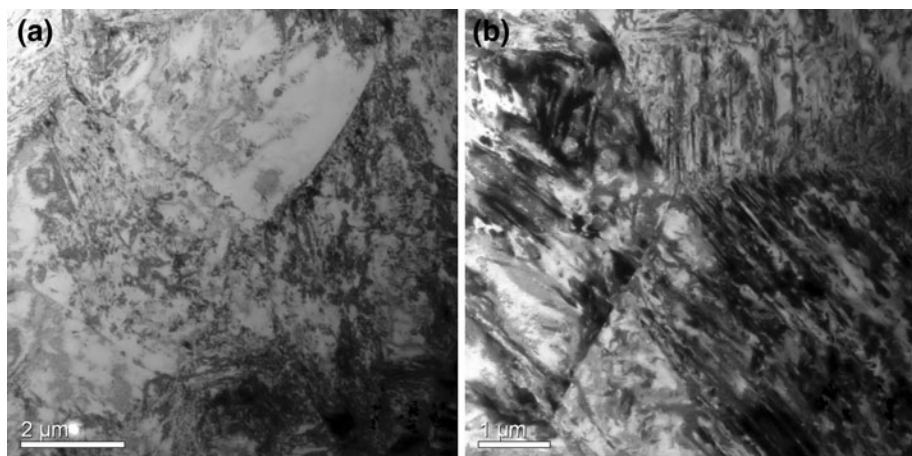


Fig. 6 TEM brightfield images of the microstructure of a 0.1 mm NiTi sheet in the as-received condition

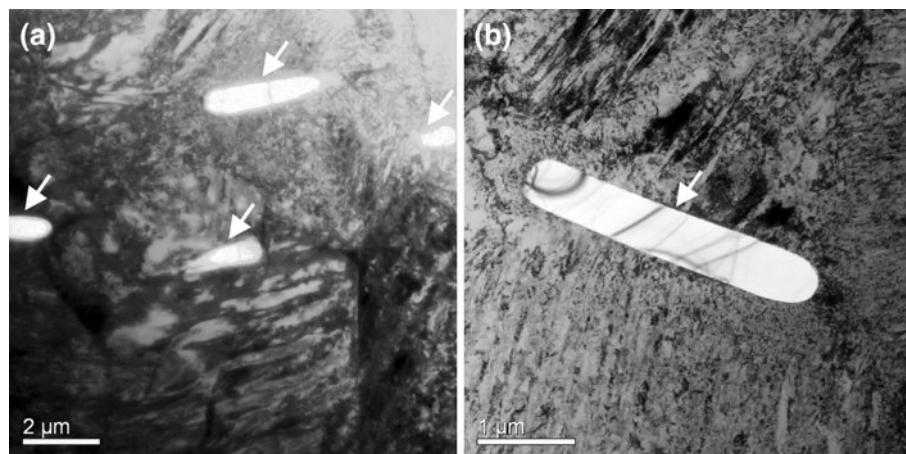


Fig. 7 TEM brightfield images of TiC particles found in the microstructure

microstructure in the as-received condition. Some high-angle grain boundaries are visible and a certain amount of grains is elongated. However, we did not observe a distinct texture as a result of the rolling process.

A variety of carbides of type TiC with different morphologies can be seen in Fig. 7 (indicated by white arrows). The

relatively high number of carbides might be one explanation for the microscopically brittle behavior during cutting, as well as for the introduction of microcracks in the NiTi matrix.

Figure 8 compares the microstructure in the as-received condition (a, b) with sheets machined with abrasive (c, d), and non-abrasive (e, f) water jet. Despite the localized plastic

deformation being visible in the SEM for the machined sheets, there appears to be no significant difference with regard to the dislocation density. However, it has to be pointed out that dislocations are hard to distinguish from grain boundaries due to the small grain size of 50-300 nm.

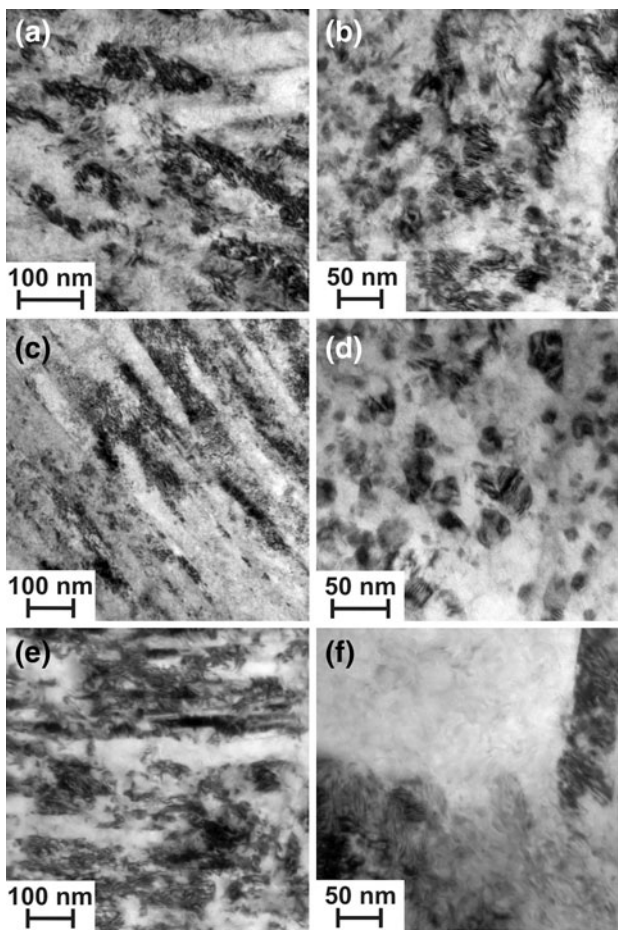


Fig. 8 TEM brightfield images comparing the microstructure of (a, b) as-received NiTi sheets with (c, d) abrasive water jet, and (e, f) non-abrasive water jet-machined sheets

The propagation of microcracks was observed in TEM-lamellae taken directly out of the cut edge of sheets machined with non-abrasive water jet, Fig. 9 (indicated by arrows). It can be seen that the cracks propagate in a transgranular way. These cracks had been visible from the surface of the cut edge in the SEM (see Fig. 5).

3.3 Micro Milling of Stent-Like Structures in NiTi Thin Sheets

In general, machining of NiTi SMA is very demanding in terms of the tool wear and the assignment of suitable process strategies (Ref 3). Earlier work has shown that only small values for the depth of cut a_p and width of cut a_c can be applied for the machining of NiTi (Ref 4). On the other hand, a larger feed rate than in macroscopic milling processes was identified as fit for the machining of NiTi. The feed per tooth related to the tool diameter is significantly larger compared to macro milling. For the machining of NiTi bulk material the literature recommends a depth of cut of $a_p = 10 \mu\text{m}$ ($0.025 \times d$), a width of cut of $a_c = 10 \mu\text{m}$ ($0.025 \times d$), a feed per tooth of $f_z = 12 \mu\text{m}$ and a cutting speed of $v_c = 19-33 \text{ m/min}$ (Ref 4). Figure 10 shows the results of the machining of circular micro pockets. The work piece quality is very good without any burr formation.

The described process strategies have to be revised to machine NiTi thin sheets. First, the sheet has to be glued to the work piece mounting to guarantee an even support over the whole structure. The choice of the tool diameter depends on the designed corner radius of the stent-like structure that is to be machined. A tool diameter of 0.4 mm is chosen to generate a minimum strut thickness of 0.2 mm. The process parameters have to be adapted in a way that allows slot milling with the complete tool diameter engaging the work piece. Thus, the feed rate has to be reduced drastically to avoid early tool failure. Compared to the water jet machining, the micro milling encounters a disadvantage in principle. Depending on the achievable depth of cut, two or more process runs are needed in order to separate the material, while laser and water jet machining processes have only one process run to perform. Figure 11 shows the microscopic view of the milling process. The struts are machined by cutting diamond-shaped sections out of the thin sheet.

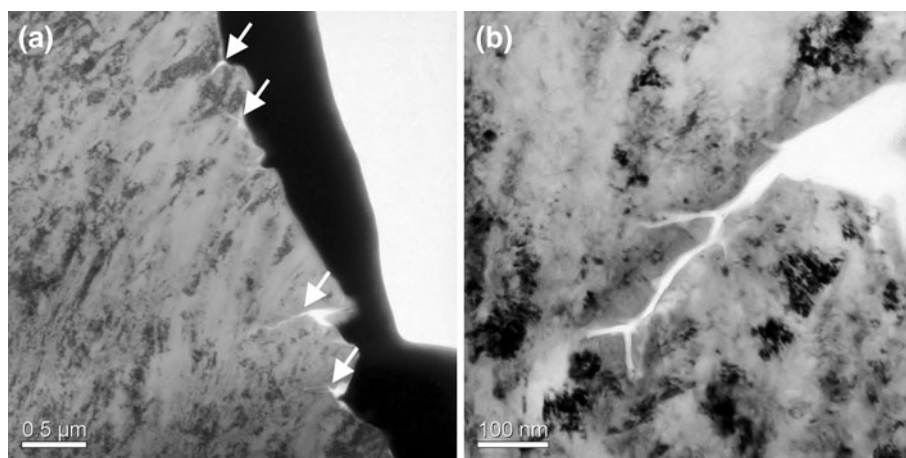


Fig. 9 TEM brightfield images showing the transgranular propagation of microcracks from the cut edge into the NiTi work piece machined with non-abrasive water jet

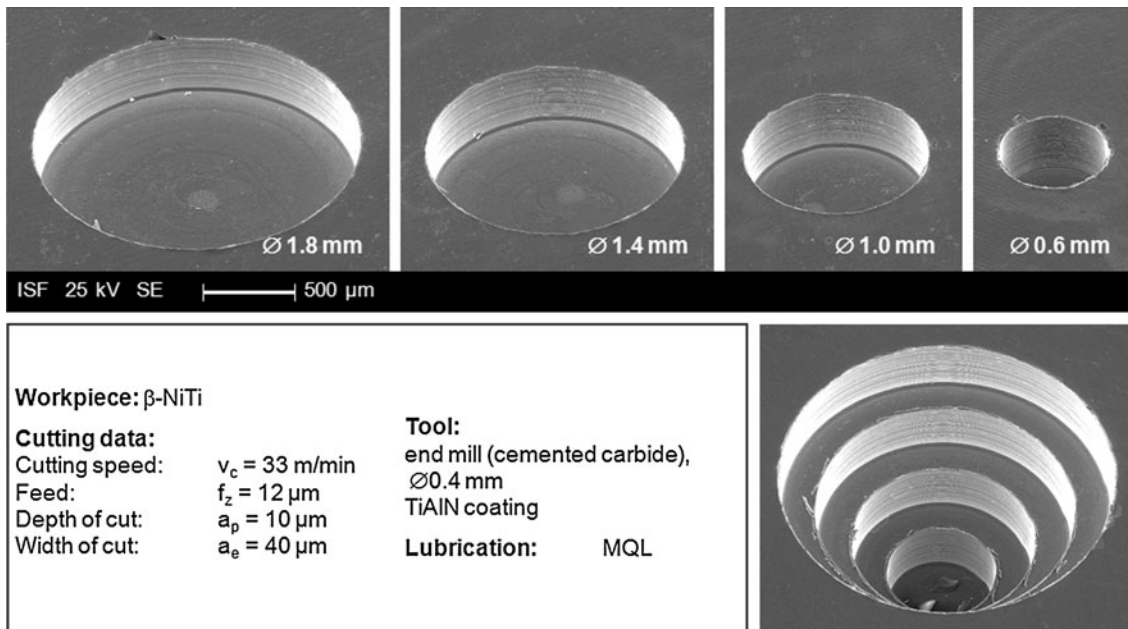


Fig. 10 Circular micro pockets in NiTi bulk material machined with end mills ($d = 0.4 \text{ mm}$)

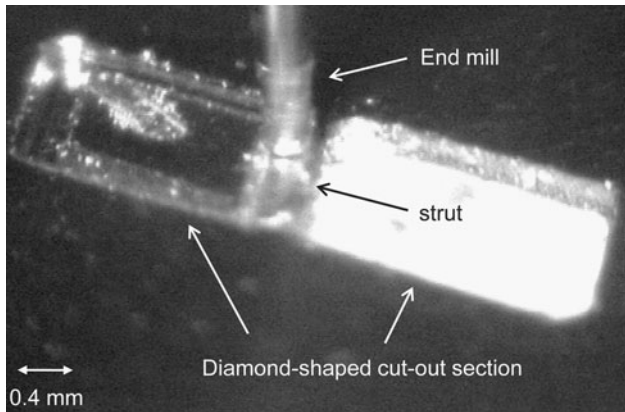


Fig. 11 Microscopic view of the micro milling process

The variation of the cutting depth of the micro milling process shows that the maximum depth of cut should not exceed $a_p = 10 \mu\text{m}$. Higher values cause a high deformation of the stent-like structure, thus reducing the shape accuracy and causing strong burr formation. A strut width of $b = 0.1\text{--}0.2 \text{ mm}$ can be achieved. Figure 12 depicts the difference of the burr formation on the front and on the backside of the structure. Especially, the backside burr depends on the depth of cut. The shown optimum occurs at a depth of cut of $a_p = 10 \mu\text{m}$ and a feed rate of $f_z = 5 \mu\text{m}$. Combinations of lower feed rates and higher depths of cut lead to an increasing burr formation.

The results show that the feed speed of $v_T = 131 \text{ mm/min}$ (10 runs) offers a good combination of a low process time and good shape accuracy for the stent-like structures. This speed means a feed per tooth of $f_z = 5 \mu\text{m}$. The cut quality of the micro machined structures depends on the milling strategy as

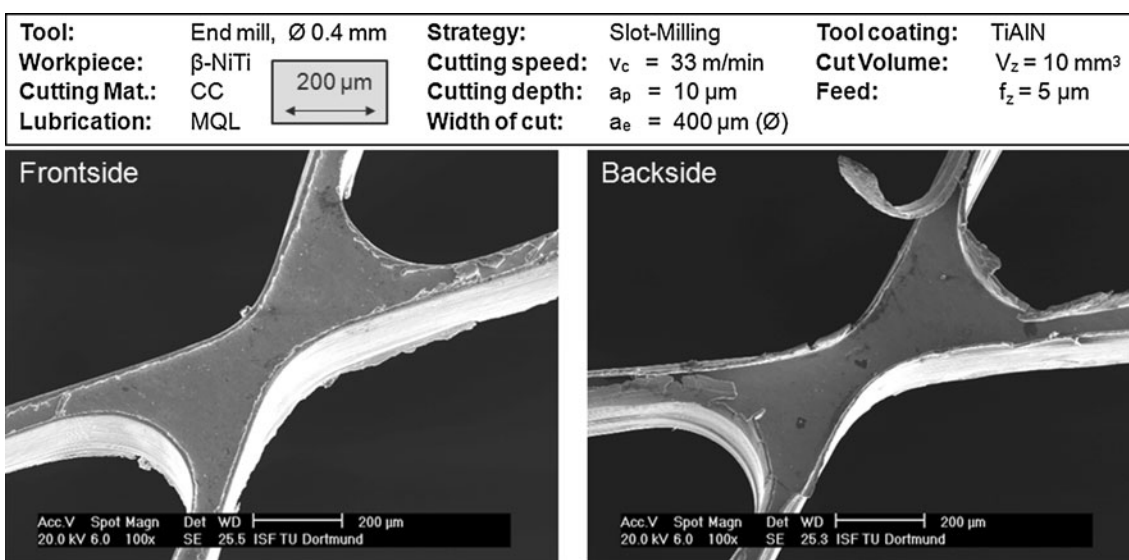


Fig. 12 Front and backside of a micro milled stent-like structure

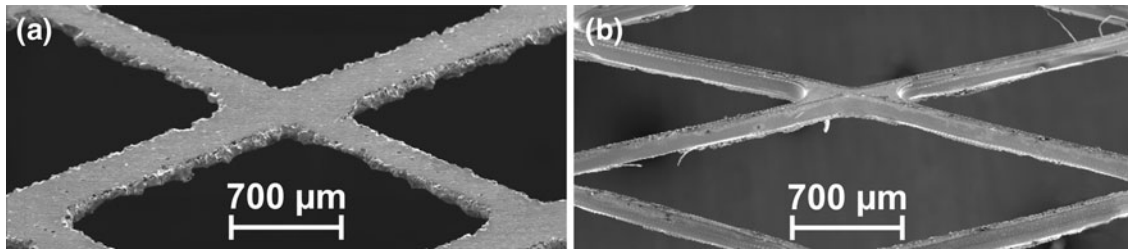


Fig. 13 Upper side of a stent-like structure machined by (a) non-abrasive water jet and (b) by micro milling

well as on the depth of cut. The slot milling contains down-milling as well as up-milling kinematics. The milling process should be designed in a way that the down-milling side of the tool is oriented toward the struts. This is mandatory in order to reduce the burr formation.

Figure 13 shows a comparison of diamond-shaped cuts, resulting in a simple stent-like structure machined by (a) water jet and (b) micro milling. It can be seen that the cut edge in (a) has a wavy nature most likely caused by vibrations of the thin sheet. A solution could be the backup of the sheet from below with a support plate featuring damping characteristics. The cut quality in (b) seems to be much better, although distinct burr formation occurs during micro milling.

4. Conclusions

The article shows an alternative approach to the cutting of thin NiTi sheets with a thickness of $s = 0.1$ mm. We demonstrate that water jet machining, as well as micro milling, are applicable processes to achieve small stent-like structures in NiTi. Water jet machining is favorably in terms of overall cutting time, thermal influence of the work piece and operating costs. However, the cutting quality is not yet sufficient and deburring or electropolishing would be required for medical applications. The advantage of micro milling is the achievable structure width of $b = 0.1$ mm. Despite the poor machinability of NiTi, good results concerning the shape accuracy of the

milled stent-like structures were obtained, whereas the burr formation still remains problematic.

Acknowledgments

The authors acknowledge funding by the German Research Foundation DFG (Deutsche Forschungsgemeinschaft) and the State North Rhine-Westphalia in the framework of projects C4, T2, T3, and Z of the Collaborative Research Center SFB459 (Shape-Memory Technology).

References

1. M. Frotscher, K. Neuking, R. Böckmann, K.D. Wolff, and G. Eggeler, In Situ Scanning Electron Microscopic Study of Structural Fatigue of Struts, The Characteristic Elementary Building Units of Medical Stents, *Proceedings of ESOMAT 2006, Mater. Sci. Eng. A*, **481–482**, 2008, p 160–165
2. A. Hascalik, U. Çaydas, and H. Gürün, Effect of Traverse Speed on Abrasive Waterjet Machining of Ti-6Al-4V Alloy, *Mater. Des.*, 2007, **28**, p 1953–1957
3. Y. Mori, S. Ishida, T. Satow, T. Konno, A. Ohkawa, and T. Honma, Mechanical Working of a TiNi Shape Memory Alloy and Its Application, *Bull. Res. Inst. Miner. Dress. Metall.*, 1987, **43**(2), p 171–178
4. V. Petzoldt and K. Weinert, Micromachining of NiTi Shape Memory Alloys, *Annals of the German Academic Society for Production Engineering, Production Engineering—Research and Development*, Vol XIII, no 2, 2006, p 43–46